UCRL--86420 Rev. 1

DE82 004385

Optical Scattering Measurements from 1.06μm, 0.53μm and 0.35μm Laser Heated Targets

R.E. Turner
E.M. Campbell
B.F. Lasinski
W.L. Mead
D.W. Phillion
F. Ze

This paper was prepared for submittal to
American Physical Society
23rd Annual Meeting
New York, N.Y.
October 12-16, 1981

October 1981

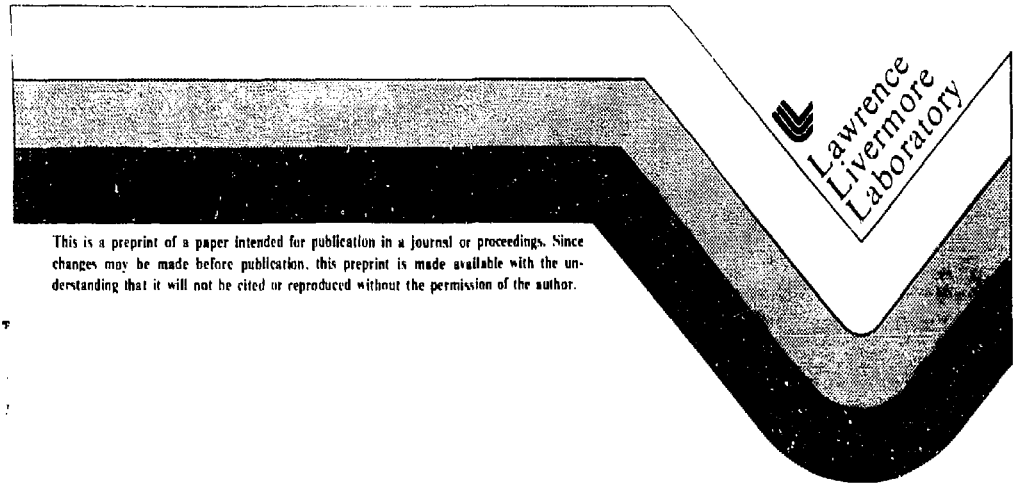

OPTICAL SCATTERING MEASUREMENTS FROM 1.06μm, 0.53μm, and 0.35μm LASER HEATED TARGETS*

R. E. Turner, E. M. Campbell, G. Hermes,

B. F. Lasinski, W. C. Mead, D. W. Phillion, F. Ze

University of California
Lawrence Livermore National Laboratory

October 1981

Abstract

Scattered light measurements have been obtained on Argus disk target experiments at 1.06μm, 0.53μm, and 0.35μm laser wavelengths. We present backscatter measurements taken near the three laser wavelengths for SBS, and measurements of the three-halves and second harmonics taken during the two longer wavelength laser irradiations. The SBS measurements show the strong influence of the increased absorption at the shorter laser wavelengths. The spectra of the three-halves harmonic emissions are analyzed to provide a time averaged electron temperature at quarter critical density. Time resolved Raman scattering data are presented for gold and Be disks irradiated with up to 180 J of green light.

---

*Work performed under the auspices of the U.S. Department of Energy by the Lawrence Livermore National Laboratory under contract #W-7405-ENG-48.

Wavelength scaling measurements, using the Argus laser system to irradiate disk targets at 1.06μm, 0.53μm, and 0.35μm, were recently completed. While the experiments concentrated on soft and hard x-ray measurements, additional diagnostics, measuring scattered light, provided information about the various processes taking place in the underdense plasma. These diagnostics included temporally and spectrally resolved measurements near; (1) the laser wavelength for stimulated Brillouin scattering (SBS); (2) wavelengths of 1.2 to 2.2 times the laser wavelength for stimulated Raman scattering (SRS); (3) and near the second and three-halves laser harmonics. All the measurements were not obtained at all 3 laser wavelengths. In particular, the high absorption at 0.35μm limited observations at that wavelength.

Electromagnetic radiation at the 3/2 harmonic of the laser frequency is indicative of plasma waves at the quarter critical density of the laser light. The harmonic may be generated by coalescence of three plasmons, or by the non-linear combining of a plasmon and an incident wavelength photon. We assume that the plasma waves are generated by the two plasmon decay instability[1].

Experimentally, at an angle of 30^0, we observe two peaks (in 1.06μm experiments), one red shifted, the other blue shifted, as shown in Figure 1. The usual[2] explanation for this is that we are observing a directly backscattered ($\theta > \pi/2$) red shifted wave, and a forward scattered ($\theta < \pi/2$) blue shifted wave which has reflected off of its critical surface (at 9/4 n_c). Evidence in support of this hypothesis

includes the following observations. The blue shifted light is reduced in amplitude compared to the red, presumably due to absorption. In 0.53μm experiments, the blue shifted light is not observed, again due to absorption. In burn through experiments on thin plastic foils, in which 3/2 light is observed in the forward direction, it is the red-shifted peak which is reduced or completely absent. Similar observations have been reported by others[3]. Other evidence, however, points out the limitations of this simple model. Three halves spectral measurements, looking for 90^{0} scattered light, should, according to equations (1) and (2) (discussed below), show only one peak. However, measurements show two well separated peaks. At this time, we do not have a unique explanation for this observation. In addition, Doppler shifts, refraction, 3 dimensional effects, the finite f-number of the focusing lens, etc. are neglected. Because of these limitations and assumptions, the temperatures derived should be regarded as model dependent.

Barr[4] gives the wavelength shift from the exact 3/2 harmonic, for a 1.06μm laser, as

$$\Delta\lambda = -33.9\ T_e\ [\cos\theta - 0.919\ ]\ (A) \qquad (1)$$

where T_e is the electron temperature in keV, and θ the angle of the scattered light with respect to the incident laser light. This equation may be derived by demanding phase matching (momentum conservation) between an incident photon and a $2\text{-}\omega_{pe}$ generated plasmon, adding

together to form 3/2 ω photon. We note that the forward scattered plasmon must have a wavenumber which is small compared to the wavenumber which is expected near threshold[1].

Avrov[2], et.al., use a model where the plasmon wavenumber is that which gives the highest 2 ω_{pe} growth rate[1], but does not allow for phase matching with an incident photon. This model gives

$$\omega\lambda = -22.7\ T_e \cos\theta \quad (A) \qquad (2)$$

for the wavelength shift away from the exact 3/2 harmonic. The higher order (but momentum conserving) process of 3 plasmon coalescence is calculated to give (within 5%) the same results.

Figure 2 shows the temperature inferred from equation (1) for Be, Ti, and Au disks irradiated at a nominal intensity of $1 \times 10^{15} W/cm^2$. Use of equation (2) would give 50% higher temperatures. The red peak-blue peak separation was used, rather than the absolute value of either peak, since this value is less sensitive to Doppler effect shifts. The absorbed energy for these shots is 16J for Be, 22.5J for Ti, and 30J for Au. This energy is partioned into heating the material, hydrodynamic expansion, and radiation. For the gold, radiative losses account for approximately 10 Joules. Hydrodynamaic losses were not measured, but are presumably highest for the low Z beryllium, and lowest for the gold. Thus, even after accounting for its radition losses, we expect gold to be hotter than the lower Z plasmas, due to its higher absorption. This expectation is confirmed by the data, although the absolute value of the temperature is somewhat lower than that predicted

by simulations, or inferred from SBS measurements. No attempt has been made to remove Doppler shift effects from the data; this requires knowledge of the velocities at both $n_c/4$ and $9n_c/4$. Since we expect the lower density to have a higher velocity, Doppler effects should cause us to underestimate the temperature. In fact, the 90^0 measurements, which are less sensitive to Doppler shifts, show a wider splitting (higher temperature) than the corresponding 30^0 meausurements.

Temporally and spectrally resolved measurements for stimulated Raman scattering (SRS) were obtained from 0.53μm laser wavelength experiments. Time-averaged spectra were obtained with finite channel detectors (5% bandwidth) for the 1.06μm experiments. We did not observe significant levels of SRS during experiments at 0.35μm. This is not unexpected, given the high absorption (> 90%) and relatively low intensities ($\leq 10^{15} W/cm^2$) of these particular experiments.

The spectra from 1.06μm experiments is qualitatively different from the spectra obtained from 0.53μm experiments. Figure 3 shows the 1.06μm experiment SRS data. This data was obtained with two (800Å channels) detectors, and compiled over 6 shots. Notice that little light was observed at wavelengths of 1.8μm or less. The peaked spectrum is consistent with the absolute Raman instability, shifted to the red as predicted by the Bohm-Gross term in the plasma wave dispersion equation, for an electron temperature of 2 to 5keV. The spectrum could also be the result of linear mode conversion of a plasma wave which has been generated by the two plasmon decay instability. This diagnostic had insufficient resolution to distinguish fine spectral details. However, there is clear evidence for plasma waves at $n_c/4$, and not at lower

densities. (Convective SRS near 1.8μm has been observed on SHIVA experiments at higher intensities and larger spot sizes.)

The SRS results from the 0.53μm experiments contrast strongly with the 1.06μm results. Figure 4 shows the time integrated spectrum from a gold disk target irradiated by 29 Joules of green light. The laser spot was highly structured, with some regions receiving intensities of well over 10^{16}W/cm^2. The spectrum shows the signature of the convective Raman instability; i.e., scattered light at wavelengths shorter than $2\lambda_0$. There is a weaker, additional scattered light signal seen at $2\lambda_0$ (1.064μm). This double peaked structure does not resemble the spectrum expected for SRS, rather, it appears similar to the 3/2 harmonic spectra (Figure 1). It may result from the re-conversion of two plasmon decay plasma waves.

Figures 5(a) and (b) show the time resolved Raman backscatter (i.e., back through the f/2 focusing lens) spectra for a gold disk irradiated with green light at an intensity of $\sim 5\times10^{15}$W/cm^2. Within the dynamic range of the streak camera (the S-1 photocathode is an order of magnitude more sensitive at 800nm than at 1064nm) only the convective instability is observed. This light is generated in the very underdense regions of the plasma: $0.05 \leq n/n_c \leq 0.16$, for $T_e \sim 3$keV and backscatter. The absolute instability may be reduced or suppressed by collisional absorption, profile steepening at $n_c/4$, or both. The time scale is correlated with the incident pulse, with zero being the peak of the incident pulse (±100psec). We observe no SRS until near the peak of the incident laser pulse; the scattering then continues until the end of the laser pulse. The delay in SRS onset may be due to the finite length

of time necessary for the plasma density scale length near $0.1n_c$ to evolve to large enough values to allow the SRS to grow. It may also be due to being below threshold until the time of the peak intensity. In this case, the observation that SRS continues for 500-800 psec, while the laser pulse intensity falls over an order of magnitude, may be indicative of filamentation.

We have observed, on some but not all of our disk experiments, a rapid (<100 psec) pulsation of the scattered light signal. This may be a signature of wave breaking, followed by re-growth of the plasma waves. Analysis of this aspect of the data has just begun.

Figure 5(c) shows the time integrated spectrum near $\omega_0/2$ for this gold disk experiment. The same double peaked spectrum as shown in Figure 4 is observed. We do not, as yet, have a quantitative explanation for this spectra.

Figures 6(a) and (b) show the time resolved SRS measurements from a Be disk irradiated at normal incidence. The spectrum and temporal behavior is qualitatively similar to the gold target results. Figure 6(c) shows the time integrated spectra near $\omega_0/2$ for a (different) Be disk, one oriented 30^0 from the laser beam (target normal in the direction of the light collector). Light near $\omega_0/2$ is not observed when the target normal is not oriented toward the light collector. This is an expected result, since refraction will cause this light to be strongly collimated. (It originates very near its own critical surface, so refractive effects are strong.)

The stimulated Brillouin backscatter (SBS) was observed at all three laser wavelengths. The results are similar, except that the intensity of

the SBS is greatly reduced as one moves to shorter laser wavelengths (see Figure 7). This is consistent with the measured increase in absorption at shorter wavelengths[5]. The Doppler shift due to plasma motion is a particular problem for SBS measurements, since the expected Doppler shift is approximately the same as the expected SBS spectral shift. We observe that the backscatter spectrum is slightly red shifted for gold targets, and slightly blue shifted for Be. If the scattering is occuring in the underdense region $n < 0.3n_c$, as expected from simulations, then the data imply slightly supersonic flow for Be and slightly subsonic flow for gold targets.

To summarize, scattered light measurements are useful laser plasma interaction diagnostics. In wavelength scaling experiments, they show the effects of increasing collisional absorption at shorter laser wavelengths. SRS and 3/2 harmonic measurements show the presence of plasma waves at $n_c/4$ and lower densities.

References

1. C.S. Liu, M. N. Rosenbluth, Phys. Fluids 19, 967 (1976).

2. A. I. Avrov, et. al., Sov. Phys. JETP 45, 507 (1977).

3. P. D. Carter, S. M. L. Sim, E. R. Wooding, Optics Comm. 32, 443 (1980).

4. H. C. Barr, Rutherford Lab. Annual Report, Sec. 8.3.3 (1979).

5. F. Le, et. al., APS Plasma Physics Meeting, New York, NY (1981).

Figure Captions

1. 3/2 harmonic spectra (a) 1.06μm laser, gold disk; (b) 1.06μm laser, Be disk.

2. Temperatures inferred from Equation (1). for 1.06μm experiments at $1 \times 10^{15} W/cm^2$. Doppler effects not deconvolved.

3. Raman light spectrum for gold disk target, 1.06μm experiment.

4. Raman light spectrum for gold disk target, 0.53μm experiment.

5. SRS spectra from gold disk target, 0.53μm experiment (a) false color contour plot of streak record. Signal at lower right is 1.06μm timing fiducial; t=0 corresponds to the peak of the laser pulse; (b) spectrally integrated time history and time integrated spectrum from (a) (sharp cut-off at 0.7μm is instrumental limit). (c) time integrated spectrum near $\omega_0/2$. Sharp peak at 1.064μm is due to residual unconverted laser light.

6. SRS spectra from Be disk target, 0.53μm experiment. (a) false color contour plot of streak record; (b) spectrally integrated time history, and temporally integrated spectrum; (c) time integrated spectrum near $\omega_0/2$ for a different Be target (see text).

7. SBS backscatter levels for various laser wavelengths. (a) gold disk targets; (b) Be disk targets.

TIME INTEGRATED 3/2 ω SPECTRUM

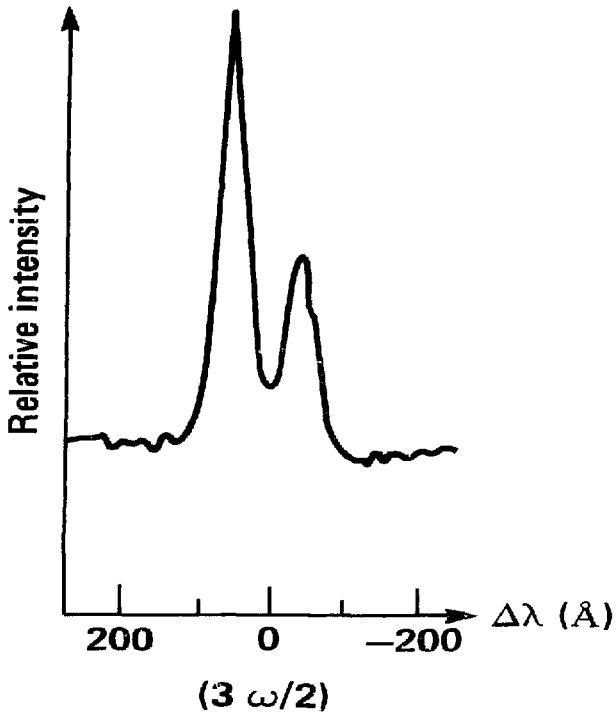

20-90-1081-3199

1.05 μm Experiment

$I = 1 \times 10^{15}$ W/cm^2 Au disk target

Red peak shifted $\approx$ 40 Å

Blue peak shifted $\approx$ 50 Å

Figure 1a

TIME INTEGRATED 3/2ω SPECTRUM

$I = 3 \times 10^{14}$ W/cm^2 Be disk target

Red peak shifted $\approx$ 30 Å

Blue peak shifted $\approx$ 20 Å

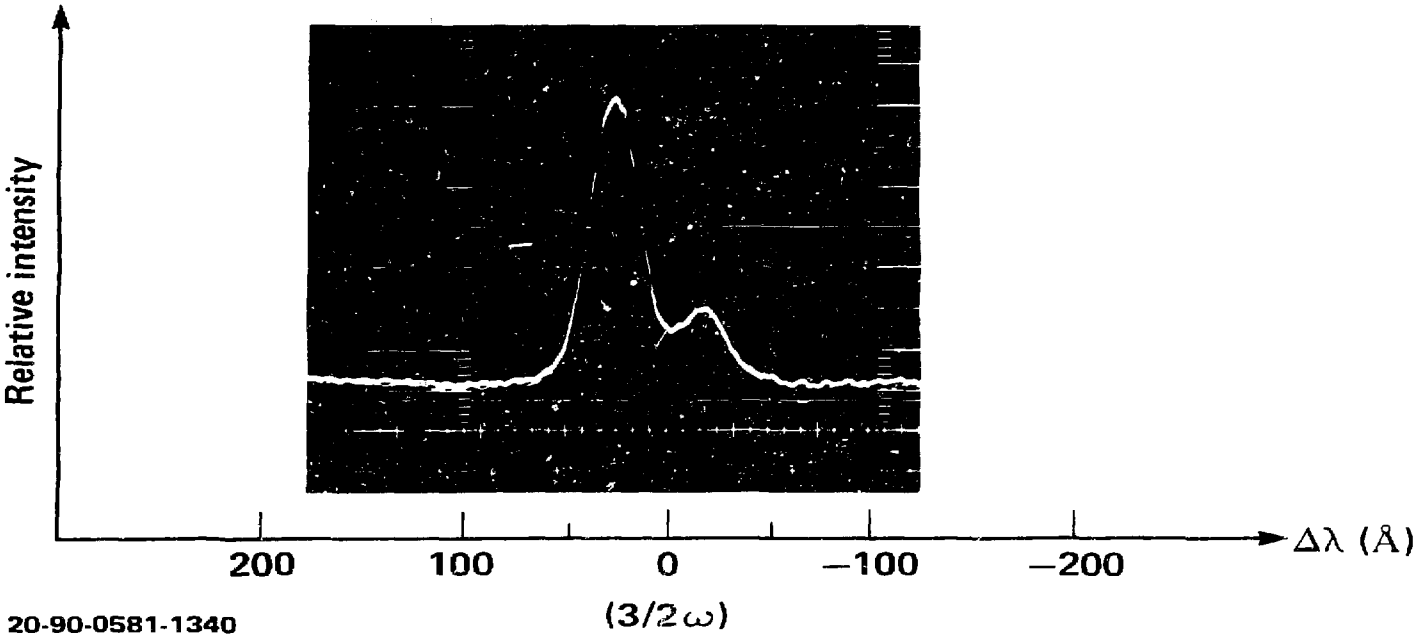

Figure 1b

ELECTRON TEMPERATURES AT $n_c/4$ INFERRED FROM 3/2 HARMONIC SPECTRAL SPLITTINGS

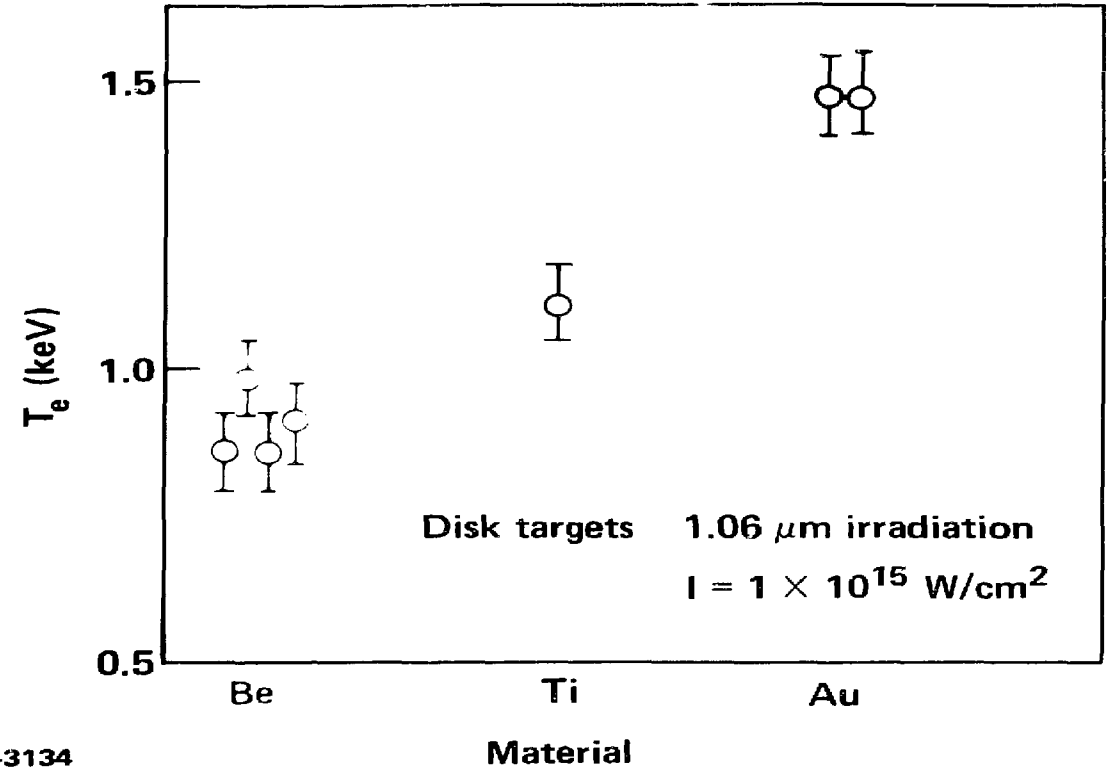

20-90-1081-3134

Figure 2

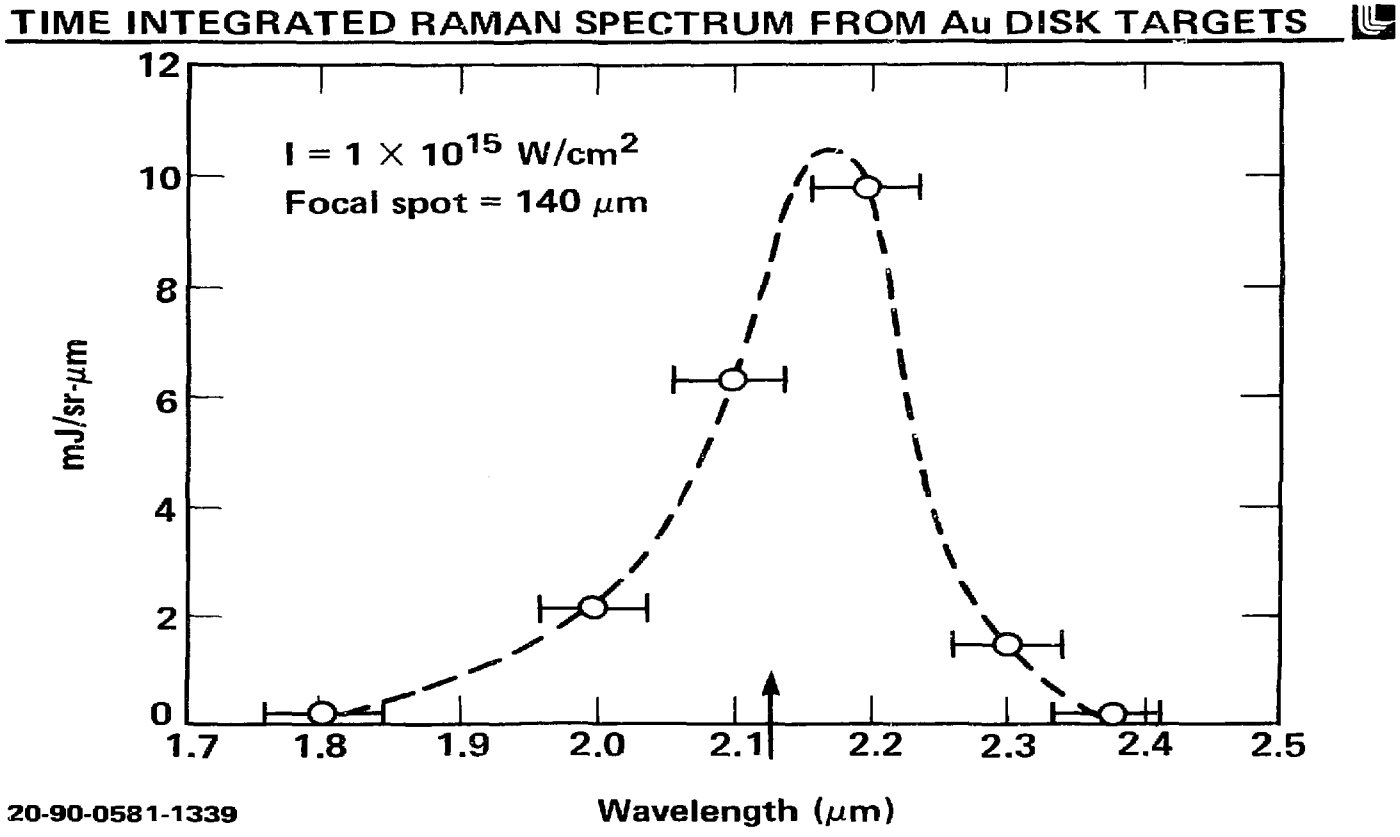
TIME INTEGRATED RAMAN SPECTRUM FROM Au DISK TARGETS
I = 1 × 10^15 W/cm^2
Focal spot = 140 μm
mJ/sr-μm
12
10
8
6
4
2
0
1.7
1.8
1.9
2.0
2.1
2.2
2.3
2.4
2.5
Wavelength (μm)
20-90-0581-1339

Figure 3

RAMAN LIGHT SPECTRUM FOR A DISK TARGET IRRADIATED WITH 5320 Å LIGHT

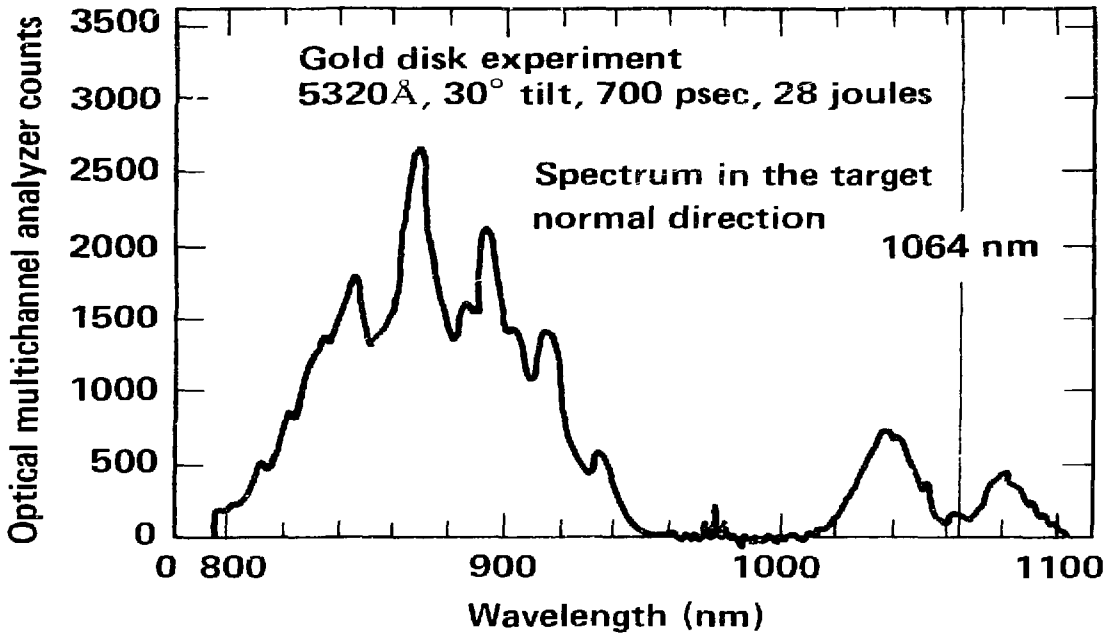

20-90-1081-3129

Figure 4

TIME-RESOLVED RAMAN-LIGHT SPECTRUM FOR A GOLD DISK IRRADIATED BY 5320 Å LASER LIGHT AT 5×10^{15} W/cm^2, 132 JOULES, 700 PSEC

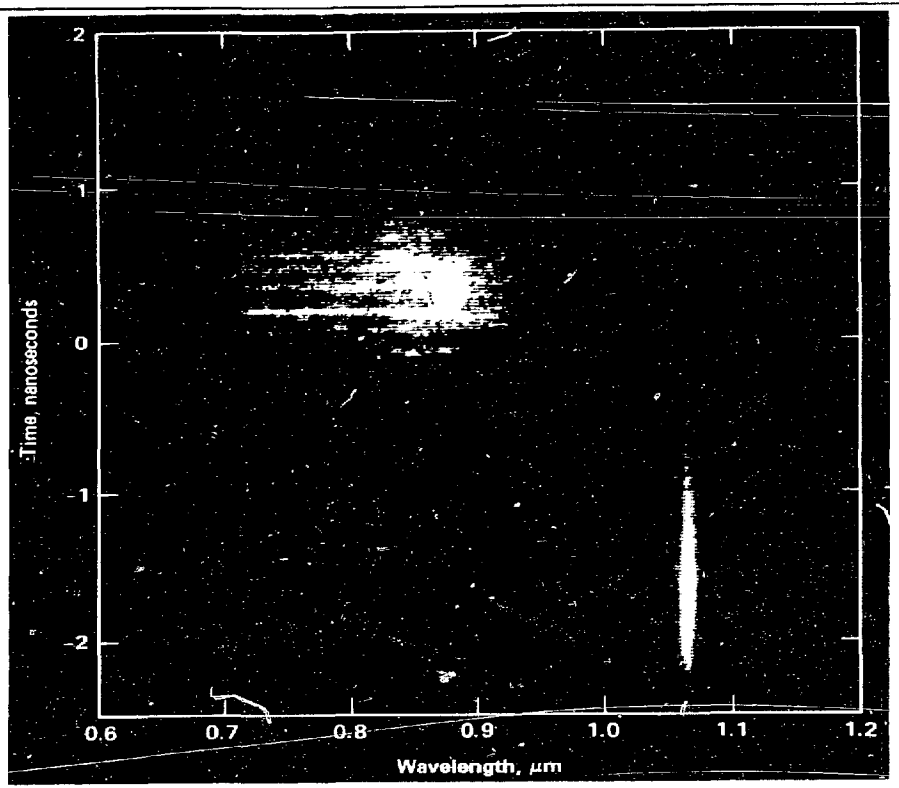

Figure 5a

TIME-RESOLVED RAMAN LIGHT SPECTRUM FOR A GOLD DISK IRRADIATED WITH 5320 Å LIGHT

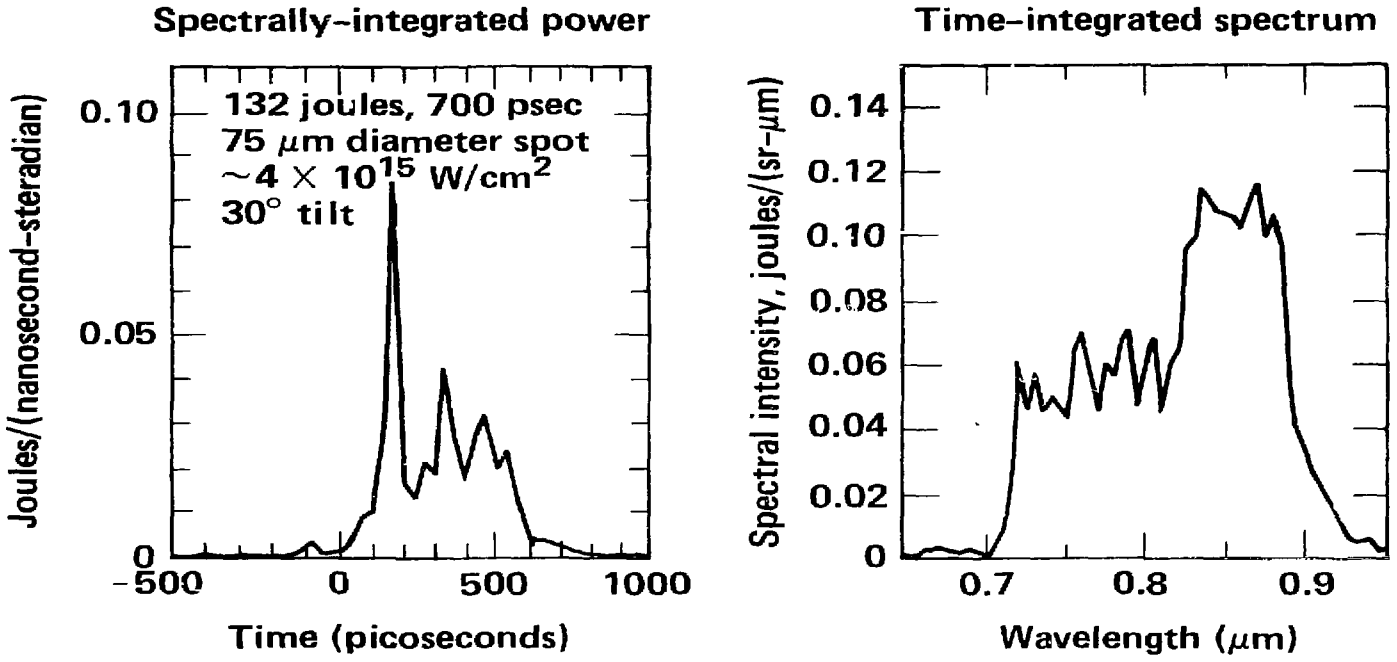

20-90-1081-3171

Figure 5b

SPECTRUM OF THE $\omega_0/2$ LIGHT FOR 5320 Å IRRADIATION OF A GOLD DISK

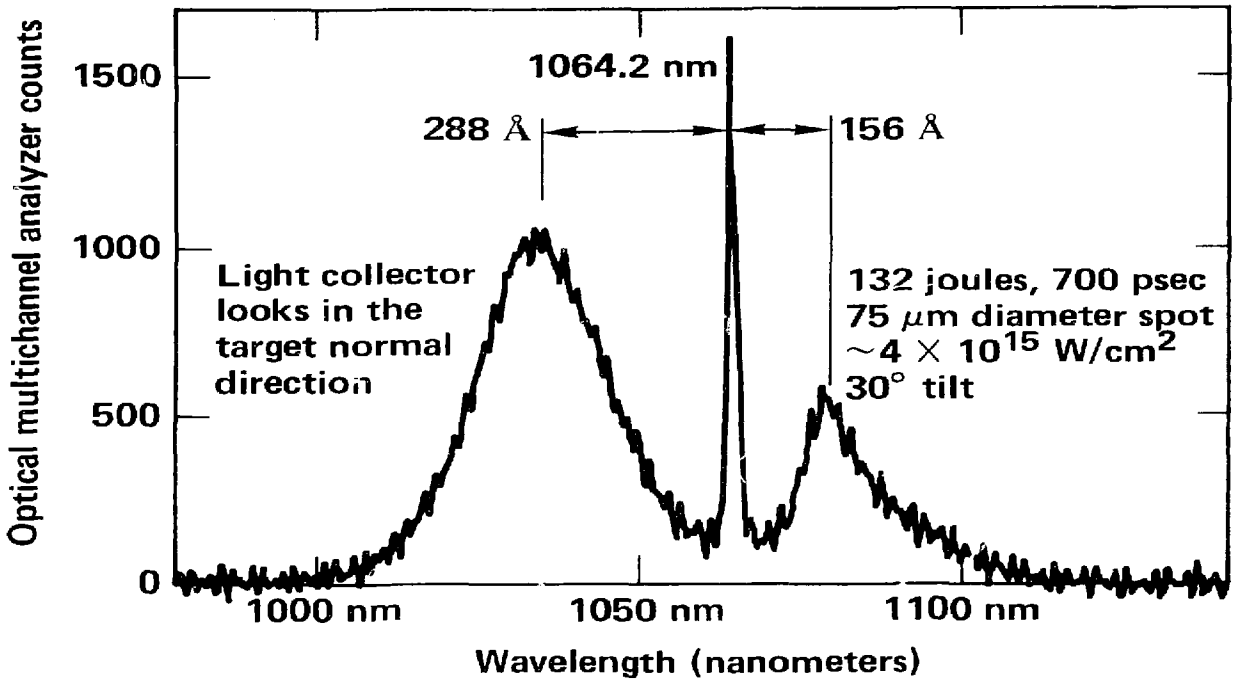

20-90-1081-3177

Figure 5c

TIME RESOLVED SPECTRUM FOR THE RAMAN LIGHT FOR 5320Å LASER IRRADIATION AT 5×10^{15} W/cm^2, 132 JOULES, 700 psec

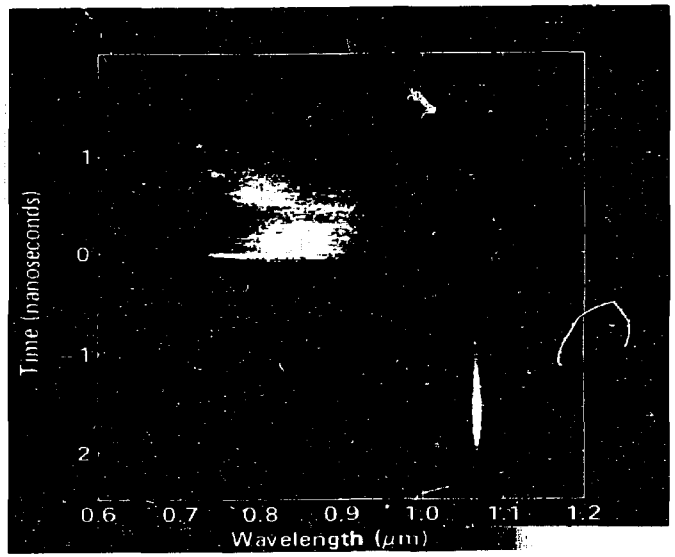

20-90-1081-3205

Figure 6a

TIME-RESOLVED RAMAN LIGHT SPECTRUM FOR A BERYLLIUM DISK IRRADIATED WITH 5320Å LIGHT

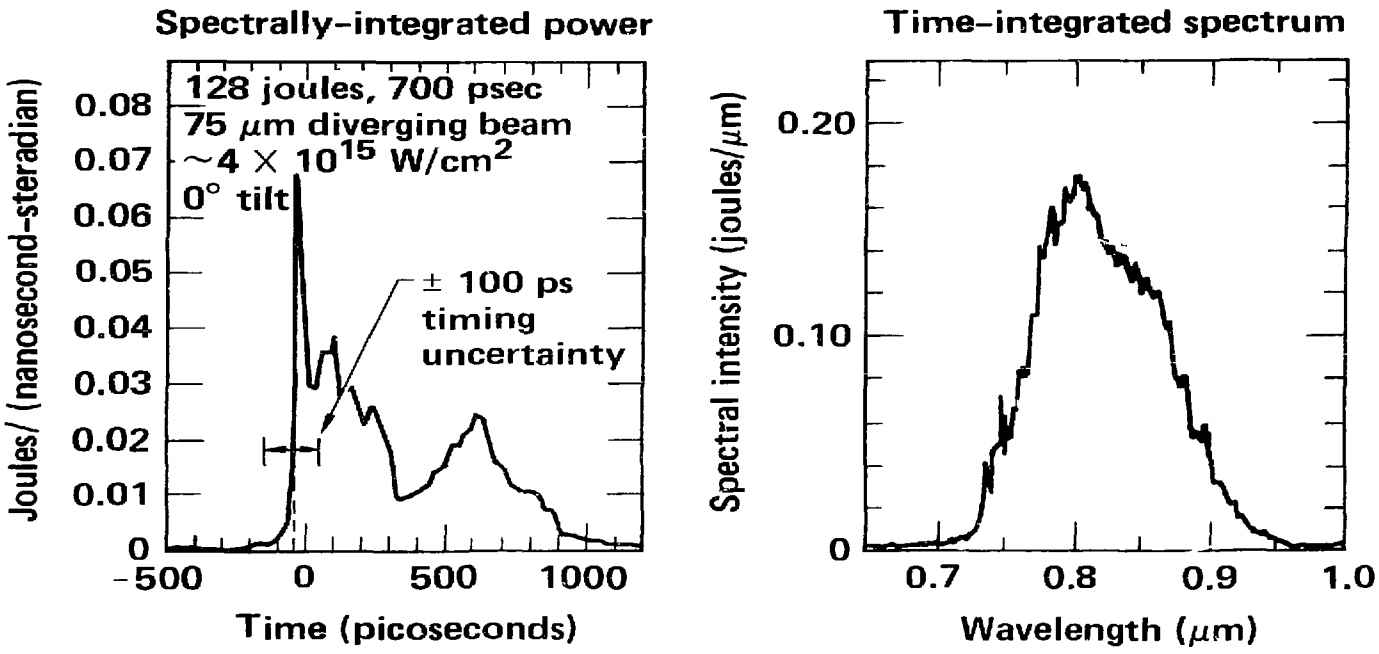

20-90-1081-3163

Figure 6b

SPLITTING OF THE $\omega_0/2$ LIGHT SPECTRUM IS MUCH LESS FOR A BERYLLIUM DISK THAN FOR A GOLD DISK FOR THE SAME IRRADIATION CONDITIONS

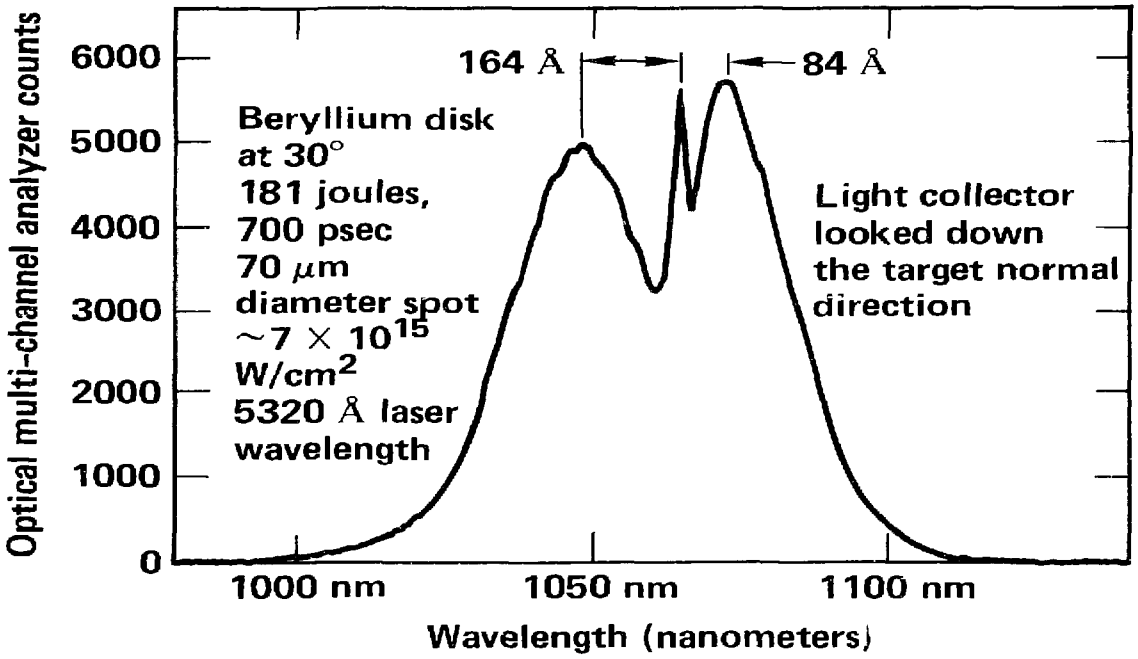

20-90-1081-3182

Figure 6c

FRACTIONAL BACKSCATTER THROUGH f/2 FOCUSING LENS

Au Disk Targets

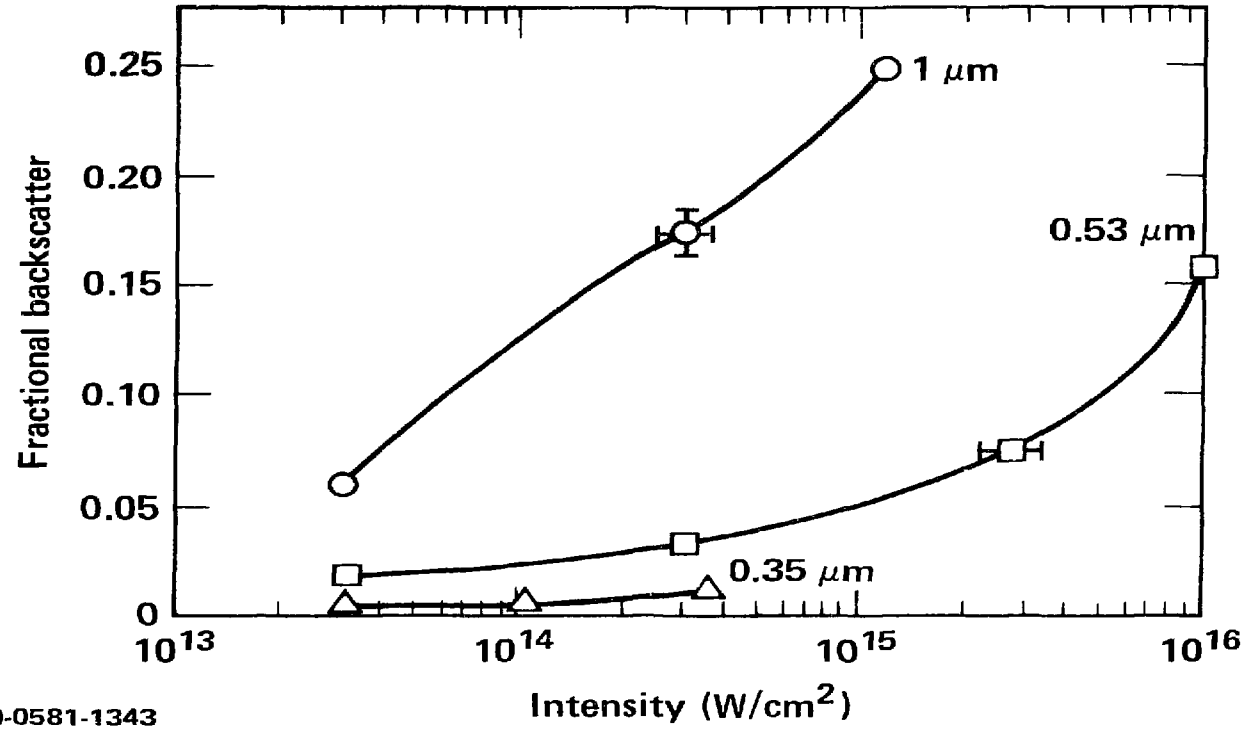

20-90-0581-1343

9/81

Figure 7a

FRACTIONAL BACKSCATTER THROUGH f/2 FOCUSING LENS

Be Disk Targets

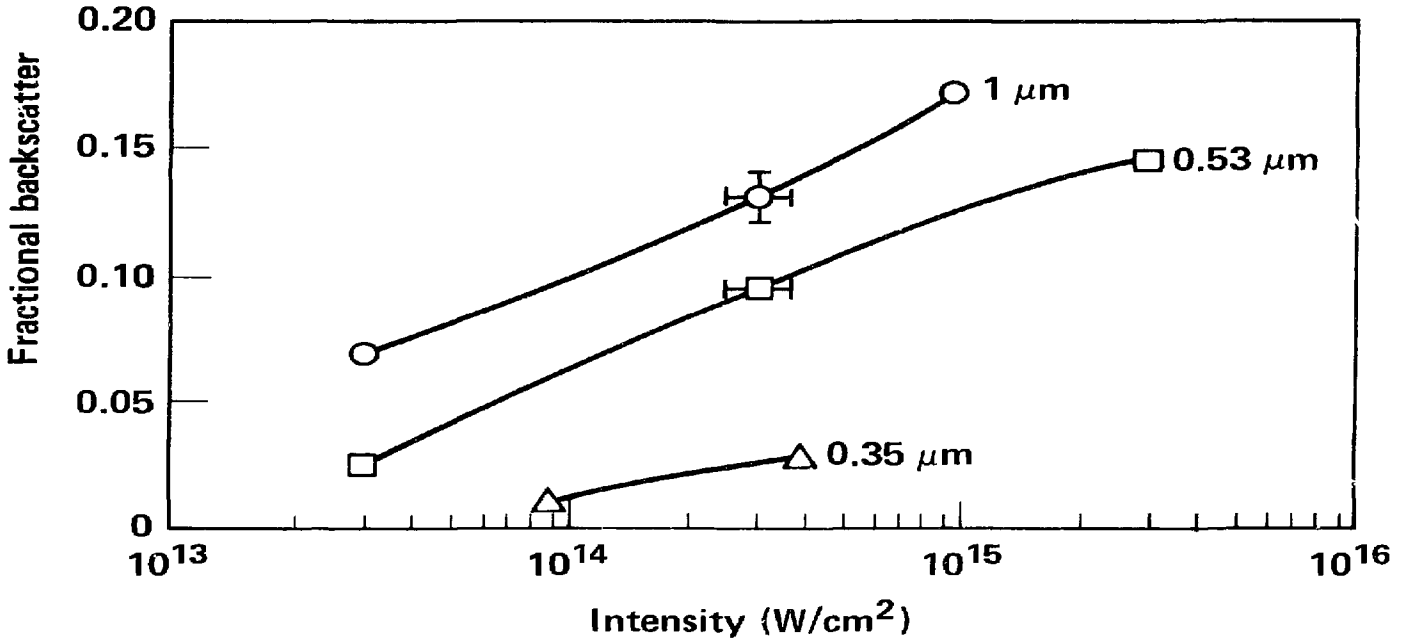

20-90-0581-1342

9/81

Figure 7b